Acta Biomaterialia 32 (2016) 10–23

Contents lists available at ScienceDirect

Acta Biomaterialia

journal homepage: www.elsevier.com/locate/actabiomat

Full length article

PNIPAAm-based biohybrid injectable hydrogel for cardiac tissue engineering

Ali Navaei [a,1], Danh Truong [a,1], John Heffernan [a,b], Josh Cutts [a], David Brafman [a], Rachael W. Sirianni [a,b], Brent Vernon [a], Mehdi Nikkhah [a,*]

[a] School of Biological and Health Systems Engineering (SBHSE), Arizona State University, Tempe, AZ 85287, USA
[b] Barrow Brain Tumor Research Center, Barrow Neurological Institute, Phoenix, AZ 85013, USA

ARTICLE INFO

Article history:
Received 13 October 2015
Received in revised form 3 December 2015
Accepted 11 December 2015
Available online 12 December 2015

Keywords:
Cell encapsulation
Gelatin
PNIPAAm
Co-culture
Cardiac fibroblast
Contraction behavior
Gene expression

ABSTRACT

Injectable biomaterials offer a non-invasive approach to deliver cells into the myocardial infarct region to maintain a high level of cell retention and viability and initiate the regeneration process. However, previously developed injectable matrices often suffer from low bioactivity or poor mechanical properties. To address this need, we introduced a biohybrid temperature-responsive poly(N-isopropylacrylamide) PNIPAAm–Gelatin-based injectable hydrogel with excellent bioactivity as well as mechanical robustness for cardiac tissue engineering. A unique feature of our work was that we performed extensive *in vitro* biological analyses to assess the functionalities of cardiomyocytes (CMs) alone and in co-culture with cardiac fibroblasts (CFs) (2:1 ratio) within the hydrogel matrix. The synthesized hydrogel exhibited viscoelastic behavior (storage modulus: 1260 Pa) and necessary water content (75%) to properly accommodate the cardiac cells. The encapsulated cells demonstrated a high level of cell survival (90% for co-culture condition, day 7) and spreading throughout the hydrogel matrix in both culture conditions. A dense network of stained F-actin fibers ($\sim 6 \times 10^4$ μm^2 area coverage, co-culture condition) illustrated the formation of an intact and three dimensional (3D) cell-embedded matrix. Furthermore, immunostaining and gene expression analyses revealed mature phenotypic characteristics of cardiac cells. Notably, the co-culture group exhibited superior structural organization and cell–cell coupling, as well as beating behavior (average ~45 beats per min, co-culture condition, day 7). The outcome of this study is envisioned to open a new avenue for extensive *in vitro* characterization of injectable matrices embedded with 3D mono- and co-culture of cardiac cells prior to *in vivo* experiments.

Statement of Significance

In this work, we synthesized a new class of biohybrid temperature-responsive poly(N-isopropylacrylamide) PNIPAAm–Gelatin-based injectable hydrogel with suitable bioactivity and mechanical properties for cardiac tissue engineering. A significant aspect of our work was that we performed extensive in vitro biological analyses to assess the functionality of cardiomyocytes alone and in co-culture with cardiac fibroblasts encapsulated within the 3D hydrogel matrix.

1. Introduction

Bioengineered injectable hydrogels enhance the efficacy of conventional cell-based transplantation for treatment of myocardial infarction [1]. Despite the minimally invasive nature of cell-based therapy, this strategy often suffers from low cell retention and lack of integration with the native myocardium [2–4]. Encapsulating exogenous cells within hydrogel-based matrices generates an ideal microenvironment for growth and retention of transplanted cells localized to the infarct region [5–7]. Although there have been significant advances in the development of these technologies, current injectable cell delivery hydrogels do not easily allow accessible tuning of mechanical robustness [8] and cell binding motifs [9,10].

To date, numerous studies have utilized different natural and synthetic biomaterials for the delivery of cells into the infarct

* Corresponding author.
E-mail address: mnikkhah@asu.edu (M. Nikkhah).
[1] These authors contributed equally to this work.

http://dx.doi.org/10.1016/j.actbio.2015.12.019
1742-7061/

region [1,11,12]. Naturally-derived materials provide bioactive sites that enable cell adhesion and migration, as well as eventual degradation of the scaffold [13–15]. In particular, fibrin, a blood component, has been used in pioneer studies as a matrix to induce angiogenesis, preserve cardiac function, and reduce infarct region expansion [16–18]. Collagen, an extracellular matrix (ECM) protein that has abundant cell-binding motifs, has also been widely used to support cell delivery and survival, retention, infiltration, and myocardium remodeling [19–21]. Matrigel [22], chitosan [7,23], gelatin [24–26], alginate [27], and ECM-derived matrices [28,29] are among other alternatives that have been used as suitable scaffolding biomaterials for myocardial regeneration and repair. Although natural based biomaterials promote sufficient cell-matrix interactions, they often suffer from batch-to-batch variability, high immunogenicity, and low tunability of ligand density and mechanical properties [30,31]. On the other hand, synthetic biomaterials, such as self-assembling peptides (SAP) [32], poly(lactic acid) and poly(glycolic acid) [33], poly(N-isopropylacrylamide) (PNIPAAm) [34–36], and poly(ethylene glycol) (PEG)-based copolymers [37] enable precise control of mechanical and chemical properties with added benefits of industrial-scale production. However, the structure of synthetic biomaterials should be further tailored to incorporate sufficient cell binding motifs. In this regard, a mixture of a synthetic based matrix and a natural hydrogel offers unique beneficial aspects for tissue engineering applications, in general, and cardiac regeneration in particular.

We aim to develop a suitable biohybrid injectable hydrogel for cardiac tissue engineering through combining a naturally-derived biopolymer with a tunable synthetic polymer. In particular, the proposed hydrogel matrix (Fig. 1) comprised of a thiol-modified gelatin (Gel-S) component to offer a desirable ECM-like bioactive scaffold with adequate cell binding motifs [24,38]. The synthetic component was a PNIPAAm-based copolymer composing of Jeffamine® M-1000 acrylamide (JAAm) and 2-Hydroxyethyl methacrylate (HEMA) [39]. PNIPAAm forms a thermosensitive injectable hydrogel [40], and JAAm increases the gel state equilibrium water content [41,42] to enhance nutrition and gas exchange [43]. After free radical polymerization of PNIPAAm, JAAm, and HEMA, the acrylation of HEMA component [39] resulted in the combination of the natural and synthetic components (PNJ-Gelatin), PNIPAAm–JAAm–HEMA (PNJHAc) and Gel-S. Prior to biological studies, the two components were mixed to initiate chemical crosslinking by Michael type reaction [44]. Subsequently, the increase in the temperature induced a physical crosslinking of the hydrogel due to the thermosensitive nature of PNIPAAm [40]. The synthesized biohybrid hydrogel ultimately featured dual chemical and thermal crosslinkability, mechanical tunability, and suitable bioactivity.

So far, most of the studies utilizing hydrogel-based matrices for cardiac tissue engineering encompass few *in vitro* analyses with mono-culture of cardiomyocytes (CMs) before *in vivo* assessments [7,8,16,18,20,21,24,33–35]. Although these studies have generated significant *in vivo* findings on the regeneration of infarcted region, we believe that there should be expanded *in vitro* investigations with co-culture of CMs and cardiac fibroblasts (CFs) to comprehensively analyze the performance of the cell-embedded hydrogel matrix prior to *in vivo* studies. Specifically, due to the abundance of resident CFs within the infarct region, it is crucial to find out whether the synthesized hydrogel is capable of accommodating CFs, and what is the subsequent role of infiltrated CFs on the overall functionalities of the formed 3D tissue [45]. Therefore, we performed extensive *in vitro* mono- and co-culture studies comprising of cell survival, cytoskeleton and cardiac-specific markers organization, gene expression, as well as tissue-level beating behavior. We hypothesize that the synthesized PNJ-Gelatin biohybrid hydrogel provides a suitable microenvironment to support the functionalities of cardiac cells, ultimately leading to enhanced repair and regeneration of injured myocardium.

2. Materials and methods

2.1. Materials

3,3′ Dithiopropionic acid (DTPA), HPLC grade tetrahydrofuran (THF), anhydrous methanol, anhydrous ethanol, acetone, hydroxylethyl methacrylate (HEMA), 2,2′-Azobisisobutyronitrile (AIBN), acryloyl chloride, hydrazine hydrate (HH), hexane, concentrated sulfuric acid, ethyl ether, 1 N hydrochloric acid (HCl), 1 N sodium hydroxide (NaOH), sodium chloride (NaCl) gelatin type A from porcine skin, N-3-dimethylaminopropyl-N′-ethylcarbodiimide hydrochloride (EDC), and 5,5′-dithiobis-2-nitrobenzoic acid (Ellman's reagent) were purchased from Sigma Aldrich (St. Louis, MO, USA). Dithiothreitol (DTT) was purchased from Gold Biotechnology (St. Louis, MO, USA). N-isopropylacrylamide (NIPAAm) was obtained from Tokyo Chemical Industry Co. (Portland, OR, USA). Jeffamine® M-1000 was gifted by Huntsman Corporation (Salt Lake City, UT, USA).

2.2. Polymer synthesis

NIPAAm monomer was recrystallized from hexane, and AIBN initiator was recrystallized from methanol. Jeffamine® M-1000 acrylamide (JAAm) was synthesized in a reaction with Jeffamine® M-1000 and acryloyl chloride [41]. Poly(NIPAAm-co-JAAm-co-HEMA), or PNJH was synthesized by free radical polymerization. Briefly, NIPAAm (7.5 g), JAAm (2 g), and HEMA (0.5 g) monomers were co-dissolved in THF, heated to 65 °C, and the reaction was initiated with AIBN (83 mg). After 18 h, the PNJH product was redissolved in acetone, precipitated in cold ethyl ether, filtered, and vacuum dried. Poly(NIPAAm-co-JAAm-co-HEMA-acrylate), or PNJHAc, was synthesized by converting hydroxyl groups on the HEMA monomer to reactive acrylates, previously reported by Heffernan et al. [39,46]. Briefly, PNJH was dried overnight at 60 °C under vacuum and then dissolved at 10 wt% in THF with TEA (2.11 mL). The reaction was initiated by adding acryloyl chloride (1.21 mL) dropwise to the stirring solution while on ice. The product was precipitated in cold ether, filtered, and vacuum dried. PNJHAc was further purified by dialysis against diH_2O (3500 MWCO) for 3 days. The lyophilized polymer was stored at −20 °C. Dithiopropionic dihydrazide (DTPH) was prepared from DTPA using an established procedure [47]. Thiolated gelatin (Gel-S) was synthesized from gelatin and DTPH using EDC chemistry based on previously reported studies [38,48]. To confirm the syntheses, proton nuclear magnetic resonance (^{1}H NMR) spectra were recorded for PNJHAc and Gel-S with D_2O as the solvent (400 MHz Varian liquid state NMR, Agilent Technologies, Santa Clara, CA, USA), while Ellman's reagent test was used to measure the degree of thiolation [49].

2.3. Preparation and physical characterization of the hydrogel matrix

To prepare the hydrogel samples for physical characterization, PNJHAc was dissolved (57.1 mg/mL) in Dulbecco's Phosphate Buffered Saline (DPBS). Subsequently, 40 mg/mL Gel-S in acidic DPBS (pH 3) was prepared at 37 °C for 5 min. The Gel-S solution was titrated with NaOH to increase the pH to 7, and then the two solutions were mixed to form the final product.

Scanning electron microscopy (SEM) (XL30 ESEM-FEG, USA) was utilized to evaluate the macroporous structure of the biohybrid hydrogels. Freshly made and hydrated (24 h at 37 °C in DPBS) samples were frozen in liquid nitrogen followed by lyophilization.

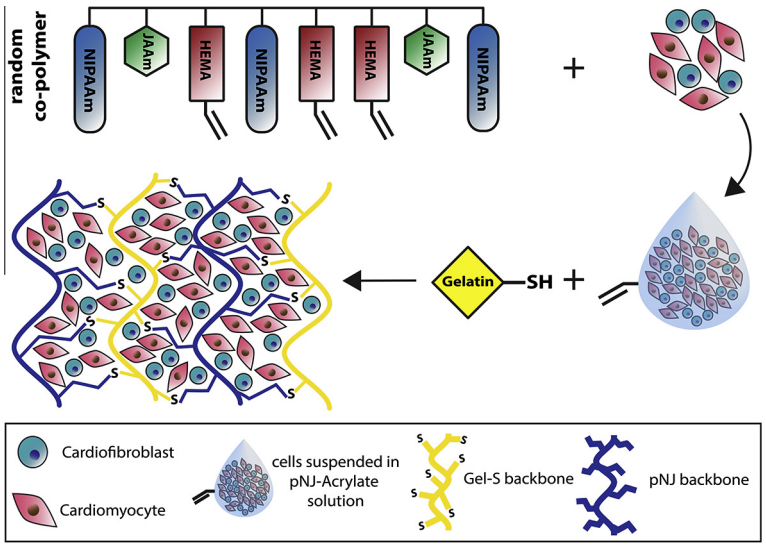

Fig. 1. The schematic displaying the fabrication procedure of the proposed injectable PNJ-Gelatin hydrogel with encapsulated CMs and CFs.

Ten SEM images were acquired to analyze the porosity and pore size distribution of the hydrogel constructs using NIH ImageJ software. Briefly, the images were thresholded and the void area was calculated. In addition, pore size was quantified using the line tool. To evaluate swelling behavior of the PNJ-Gelatin biohybrid, hydrogel constructs were prepared and immediately soaked in vials of 5 mL DPBS and relocated at 37 °C for 48 h. The swollen hydrogels were removed at different time points and weighed. The swelling ratio defined as below (Eq. (1)):

$$\textit{Swelling ratio} = \{(M_{wet} - M_{dry})/M_{dry}\} \quad (1)$$

where, M_{wet} is the mass of hydrated hydrogel and M_{dry} is the mass of fresh hydrogel. Three identical samples were selected for each time point. Rheology was completed to quantify the viscoelastic characteristics of the temperature responsive polymer during both chemical (Michael-addition induced) and physical (temperature induced) crosslinking. Rheology solutions were prepared by separately dissolving PNJHAc (57.1 mg/mL) and Gel-S (40 mg/mL) in pH 3 DPBS. The solutions were then combined, titrated to ~pH 7 with 1 N NaOH, vortex mixed for 15 s, and positioned on a parallel plate rheometer (Anton Paar MCR-101). The storage and loss modulus in the solution and gel states were evaluated by a multistep temperature controlled procedure. In the first step, a time sweep was performed for 4 h at 25 °C to measure the gelation of PNJHAc and Gel-S. Next, the sample was subjected to controlled (0.5 °C/min) and sustained heating (37 °C for 1 h) followed by quick cooling back to room temperature (25 °C for 1 h) to measure the reversible physical crosslinking of the PNJ-Gelatin hydrogel. To simulate the biophysical cues that cultured cardiac cells sense during the preparation and the first 12 h of culture, we performed a separate rheology measurement at 25 °C for 15 min (the sample preparation time) followed by immediate temperature increase to 37 °C for 12 h. In all experiments, an oscillatory 0.5% shear strain deformation was performed a frequency of 1 Hz, and normal force control was utilized to maintain constant contact between the gel and rotating head.

The LCST of PNJ-Gelatin following enzymatic digestion with collagenase was evaluated by cloud point measurement. PNJ-Gelatin was dissolved at 0.1 wt% in PBS at pH 7.4 in cuvettes and heated in a water bath from 25 to 37 °C in 1 °C increments and 40–75 °C in 5 °C increments. Samples were maintained at each temperature for at least 120 s before each measurement. Absorbance at 450 nm was recorded with a UV/Vis spectrometer (Pharmacia Biotech Ultrospec 3000). The LCST, which is defined as the temperature at 50% of the maximum absorbance, was then collected.

To assess hydrolytic degradation, hydrogel constructs were prepared and immediately placed in vials of 5 mL DPBS at 37 °C. At different time points, constructs were immersed in liquid nitrogen, followed by lyophilization. Remaining mass percentage was defined as the lyophilized mass to the original one. Three identical samples were selected for each time point.

2.4. Cell harvesting and culture

Neonatal rat ventricular CMs were isolated from 2-day old pups according to the previously established protocol [50] accepted by the Institution of Animal Care at Arizona State University. The isolated cardiac cells were separated into CMs and CFs by pre-plating the cell suspension for 1 h and allowing CFs to attach to the tissue culture flask, due their higher adhesive nature compared to CMs [50,51]. After 1 h, the harvested media, mainly containing CMs, was collected and used for further experimentation. We precisely isolated the ventricular tissue to minimize the presence of endothelial or smooth muscle cells, from the aorta region of the heart, within the isolated CMs population. However, the isolated CMs may still contain a few number of endothelial cells due to the presence of capillaries within the myocardial tissue. CMs and CFs were cultured in cardiac media containing Dulbecco's modified eagle medium (DMEM) (Gibco, USA), 10% fetal bovine serum (FBS) (Gibco, USA), L-Glutamine (1%) (Gibco, USA), and 100 units/mL of penicillin–streptomycin. Isolated cardiac cells were cultured under a static condition (no external electrical stimulation) and the cell culture media was changed every other day.

2.5. Preparation of the biohybrid cell-laden hydrogel

To prepare the cell-laden injectable PNJ-Gelatin biohybrid hydrogel, CMs (mono-culture condition) or a 2:1 ratio of CMs-CFs (co-culture condition) were dispersed (35×10^6 cells/mL) in a solution of supplemented cardiac media containing 30% FBS and PNJHAc (57.1 mg/mL). Next, a 7.5 μL drop of cardiac cell suspension was placed on top of a sterile 18×18 mm^2 glass slide. Subsequently, a 7.5 μL Gel-S in cardiac media prepared at 40 mg/mL was mixed with the cell suspension with a final cell number of 525,000 CMs in mono-culture and 350,000 CMs and 175,000 CFs in co-culture conditions (Fig. 1). The prepared samples were

chemically crosslinked in a 24-well plate at room temperature (25 °C) for 10 min followed by the addition of 0.5 mL of warmed cardiac media (37 °C) to initiate the physical crosslinking. The well plates were placed in humidified cell culture incubator (37 °C and 5% CO_2) and subsequently cultured for a period of 9 days.

2.6. Cell viability assay

The survival of encapsulated cells within the PNJ-Gelatin hydrogel was evaluated on day 1 and 7 of culture, using a Live/Dead assay kit (Life technologies, USA) and following manufacturer protocol. Briefly, three individual samples of biohybrid hydrogels were selected for each type of culture (mono- and co-culture) and Z-stack fluorescent images were acquired using an inverted microscope (Observer Z1, Zeiss, Germany) equipped with ApoTome.2 (Zeiss, Germany). The viability percentage was defined as number of viable cultured cardiac cells (green) divided by total number of cells.

2.7. F-actin staining and Fast Fourier Transform (FFT) analysis

F-actin fibers were stained to visualize the cytoskeleton organization of cultured cells within the PNJ-Gelatin hydrogel in both mono- and co-culture groups on day 7 of culture. First, the cells were fixed in 4% paraformaldehyde (PF) for 30 min. Next, 1% (v/v) Triton x-100 was used to permeabilize the plasma membrane of the cells for 45 min at 25 °C. Afterwards, the fixed cells were blocked in 1% (v/v) bovine serum albumin (BSA) (Sigma-Aldrich, USA) for 1 h at 4 °C. Finally, the cells were stained with Alexa Fluor-488 phalloidin (1:40 dilution in 1% BSA, Life technologies, USA) for 1 h and counterstained with 4′,6-diamidino-2-phenylindole dihydrochloride (DAPI, 1:10,000 dilution) for 30 min. A fluorescent microscope equipped with ApoTome.2 was utilized to take Z-stack fluorescent images through the samples. FFT images were further obtained and analyzed by means of ImageJ software (NIH) to assess the local organization of the F-actin fibers. To analyze the actin coverage area, the collected regions of interests, (ROIs) ($300 \times 300\ \mu m^2$), were quantified using NIH ImageJ software ($n > 10$).

2.8. Immunostaining of cardiac specific-markers

To investigate the phenotype of cultured cardiac cells (on day 7 of culture), immunostaining method was utilized according to previously developed protocols [26]. Briefly, cells were fixed in 4% PF for 40 min followed by treatment with 0.1% Triton x-100 for 45 min at room temperature. Next, the cardiac cells were blocked in 10% goat serum for 2 h at 4 °C. Afterwards, the fixed cells were stained with primary antibodies against sarcomeric α-actinin, connexin 43 (Abcam, USA) and troponin I (Developmental Studies Hybridoma Bank) (1:100 dilution in 10% goat serum) and placed in cold room (4 °C) for 24 h. After the primary staining, samples were washed five time with DPBS (5 min intervals) and stained overnight with secondary antibodies (Life Technologies, USA) comprised of Alexa Fluor-488 for sarcomeric α-actinin and troponin I, and Alexa Fluor-594 for connexin 43 (1:200 dilution in 10% goat serum). Next, cells were stained with DAPI (1:10,000 dilution in DPBS) for 30 min to label the nuclei. Finally, the stained samples were mounted and imaged (20× and 40×) using a ZEISS fluorescent microscope equipped with ApoTome.2. The average coverage area ($n > 12$) for cardiac-specific proteins was assessed similar to F-actin coverage analysis using NIH ImageJ software.

2.9. Quantitative polymerase chain reaction (QPCR)

QPCR technique was used to evaluate the expression of certain cardiac specific genes (CTNT, CX43, ACTN1, and MLC2v) for both culture groups. Samples were selected at two considered time points (day 1 and 7 of culture encapsulated within the PNJ-Gelatin hydrogel). For cell-laden matrices, the hydrogels were immersed in collagenase (Worthington Biochemical Corp., USA) solution (1 mg/mL) for 1 h at 37 °C to collect the encapsulated cardiac cells. After degradation of the hydrogel, the cell suspension was centrifuged at 1000 rpm for 5 min and the resulting supernatant was discarded. In the case of freshly isolated cells, the cell suspension was centrifuged at 1000 rpm for 5 min. RNA was isolated from cells using the NucleoSpin® RNA Kit (Clontech). Reverse transcription was performed with iScript Reverse Transcription Supermix for RT (Biorad). Quantitative PCR was carried out using TaqMan® Assays or SYBR® green dye on a BioRad CFX384 Touch™ Real-Time PCR Detection System. For the QPCR experiments run with TaqMan® Assays, a 10 min gradient to 95 °C followed by 40 cycles at 95 °C for 5 s and 60 °C for 30 s min was used. For QPCR experiments run with SYBR® green dye, a 2 min gradient to 95 °C followed by 40 cycles at 95 °C for 15 s and 60 °C for 1 min was used. Gene expression (Table S1) was normalized to 18S rRNA levels. Delta C_t values were measured as $C_t^{target} - C_t^{18s}$. All experiments were accomplished with two technical replicates and three biological replicates. Relative fold changes in gene expression were quantified using the $2^{-\Delta\Delta C_t}$ technique [52]. Data were presented as the average of the biological replicates ± standard error of the mean (SEM). The primers used for qPCR analysis are listed in supplementary Table S1.

2.10. Evaluation of spontaneous tissue-level contraction

The spontaneous beating of CMs was monitored and measured every day during the culture period (9 days) using real-time optical microscopy. After detection of synchronous tissue-level ($2.5 \times 2.5\ mm^2$) beating, videos ($n > 12$) were captured by using an inverted microscope equipped with an AxioCam MRm camera (Zeiss, Germany). Furthermore, representative beating signals were acquired using a custom written MATLAB code [51]. The amplitude and frequency variation indexes were calculated based on an original procedure developed by the authors. In detail, the collected beating signals of subsets ($n = 5$, $0.5 \times 0.5\ mm^2$) for each sample ($n = 4$, $2.5 \times 2.5\ mm^2$) were processed using MATLAB software to find the significant peaks. A significant peak was defined as below:

$$Significant\ peaks \geq (|Amp_{Median} - Amp_{Mean}| + Amp_{Mean}) \quad (2)$$

where Amp_{Median} and Amp_{Mean} were the median and mean amplitudes respectively. Next, the collected significant peaks ($n > 500$) were normalized based on their average. The absolute difference between the normalized values and 1 was calculated to obtain the amplitude variation index. In the case of the frequency variation index, the related time for each significant peak was acquired and peak-to-peak time differences were calculated. Subsequently, the time differences were normalized to their average and the absolute difference between the normalized values and 1 was considered as the frequency variation index. Finally, the calculated indexes ($n > 20$) were compared between mono- and co-culture groups.

2.11. External electrical stimulation

The response of the encapsulated cells (CMs and CFs), within the PNJ-Gelatin hydrogels, to external electrical stimulation was evaluated based on previously established protocol [53]. Briefly, a custom made chamber was assembled using two carbon electrodes (5 mm) with 1 cm spacing attached to a plastic petri dish (6 mm diameter) by silicon adhesive (Fig. S3A). Platinum wires were connected to the carbon electrodes (at the opposite ends of each

electrode) and all connections were sealed using silicon adhesive. The entire chamber was washed with ethanol (70%) and put under UV light for 1 h for sterilization. To assess cardiac cells' response to the external electrical stimulation, pulsatile electrical signals (BK PRECISION 4052) with 3 ms duration at three different frequencies (1, 2, and 3 Hz) was applied in both mono- and co-culture conditions. The minimum required voltage to obtain contraction of CMs was defined as the excitation threshold.

2.12. Statistical analysis

The data was analyzed using t-test and ANOVA statistical methods. The results for viability, cytoskeleton, and cardiac specific markers coverage areas were reported as mean ± standard deviation (SD). To determine a statistically significance difference between the groups, we used Tukey's multiple comparison test, with a p-value < 0.05 considered to be significant. All the statistical analyses were performed by GraphPad Prism software (v.6, GraphPad San Diego).

3. Results

3.1. Preparation and characterization of PNJ-Gelatin hydrogel

The PNJ-Gelatin hydrogel was obtained by mixing PNJHAc and Gel-S pre-polymer solutions at room temperature, which resulted in an orange solution followed by forming a soft gel after 120 s. Fig. 2A shows the viscoelastic characteristics of the hydrogel during the chemical crosslinking between PNJHAc and Gel-S. As can be seen in the graph, the storage modulus (G′) increased over time and leveled out at approximately 4 h, indicating completion of chemical crosslinking. There was a sharp increase in G′ (870 Pa) within the first hour of crosslinking, followed by a gradual increase to 1260 Pa up until 4 h. Furthermore, the hydrogel mainly exhibited elastic-behavior due to the negligible loss modulus (G″, 19 Pa after 4 h). To further investigate the impact of the thermosensitivity of the NIPAAm component, the dynamic modulus was measured during a temperature ramp from 25 °C to 37 °C. As shown in Fig. 2B, the rise in temperature induced an increase in the dynamic modulus of the PNJ-Gelatin hydrogel from 1260 to 2450 Pa, which indicated the occurrence of physical crosslinking. The dual-crosslinking (chemical and physical) nature of the biohybrid hydrogel was confirmed by dropping the temperature to 25 °C (Fig. 2C), which resulted in the same storage modulus (4 h) shown in Fig. 2A. Furthermore, the simulated rheology measurement (Fig. 2D) revealed that the cultured cells initially experienced a slight increase in the modulus up to 90 Pa within the first 15 min. Upon temperature increase occurring from the placement of the hydrogel samples in the incubator, the modulus increased as expected due to the crosslinking of PNIPAAm. To investigate the fate of the LCST after degradation of the gelatin, the PNJ-Gelatin hydrogel was degraded utilizing collagenase and cloud point measurements were taken of the degraded PNJ-Gelatin. The results indicated that LCST was 55 °C (supplementary Fig. S1) after enzymatic degradation, which is a temperature outside of physiological range. Therefore, it could be possible to utilize this degradation mechanism similar to previously developed degradable PNIPAM-based hydrogels [54].

Fig. 3A illustrates the level of water content within the hydrogel constructs. Initially, the hydrogels swelled to 1.2 times their initial mass. After 48 h, hydration decreased to a stable level of 80%. Moreover, to investigate the macroporous architecture of the PNJ-Gelatin constructs, samples were characterized by SEM before and after hydration (24 h). Fig. 3B displays the hydrogel porosity percentage as an indicator of void spaces within the constructs. As can be seen, the porosity percentage slightly increased after hydration from 71.1% ± 1.5 to 75.6% ± 2.4. Furthermore, based on the SEM images (Fig. 3C and D), the macroporous structures appeared to collapse and disorganize before hydration; however, once hydrated, morphology of the pores became more open, intact, and organized. These findings indicated that the absorbed water penetrated throughout the construct and inflated the pores. It was speculated that the average pore diameter would increase due to the higher hydration content, however no differences were observed (data not shown). Instead, the pore size distribution range expanded after hydration while maintaining the same average pore diameter (Fig. 3E).

3.2. Three-dimensional (3D) cell culture and survival

To demonstrate the capability of the PNJ-Gelatin hydrogel as a 3D microenvironment promoting cardiac cell adhesion, spreading, and survival, we encapsulated CMs (mono-culture) and a 2:1 ratio of CMs-CFs (co-culture) within the hydrogel matrix for a period of 9 days. We selected this ratio of CMs to CFs based on our recent study where we found the best viability, cell spreading and tissue-level functionalities [50]. Z-stack images (Fig. 4A) confirmed successful fabrication of a homogenous 3D (150 μm thick) construct. Fig. 4B illustrates the changes in cell morphology as a function of time regardless of culture type. Phase contrast and fluorescent images were used to highlight the cell morphology (Fig. 4B) as well as cell viability (Fig. 4C). Both cell types encapsulated within the hydrogel matrix adopted a round morphology on day 1 of culture (Fig. 4B). The synthesized matrix supported the gradual spreading of both cells in the two culture conditions as a function of time. However, on day 4, the co-culture group demonstrated a higher number of elongated cardiac cells, whereas mono-culture mostly exhibited cells with round morphology (supplementary Fig. S2). In addition, round and elongated cardiac cells formed clusters in the co-culture group in comparison to separated arrangements of the cells in the mono-culture. By day 7, the CMs and CFs in the both culture groups exhibited higher numbers of elongated and spread cells in comparison to the first day (Fig. 4B). In particular, CFs demonstrated a larger cell area (Fig. 4B, co-culture inset #1) compared to CMs (Fig. 4B, mono-culture inset & co-culture inset #2). Interestingly, CMs in the co-culture exhibited small protrusions, which were rarely seen in mono-culture (Fig. 4B, co-culture inset #3 & 4). Overall, the cells exhibited well-connected structures in co-culture condition as compared to the mono-culture. Fig. 4C represents the quantitative results of the cell viability where both culture groups exhibited high levels of cell survival. Particularly, mono- and co-culture groups resulted in approximately 80% overall cell viability on day 1, while the average overall cell viability increased to 85% for mono-culture and 90% for co-culture by day 7. There were no statistically significant differences among the culture days for mono-culture. In contrast, due to the proliferative nature of CFs [50,55], co-culture group exhibited an increase in overall cell viability (t-test (two tailed); $p < 0.05$).

3.3. Assessment of cytoskeleton organization

F-actin fibers were stained on day 7 of culture to determine the cytoskeleton organization and morphology of the cells in mono- and co-culture groups. Co-culture of the cells produced an intact and dense organization of cytoskeleton (F-actin) compared to mono-culture, which exhibited a discrete and loosely packed arrangement of F-actin fibers (Fig. 5A). These observations were consistent with phase contrast images demonstrating pronounced network of connected cells in the co-culture condition. Furthermore, FFT analysis was performed on 20× and 40× images to

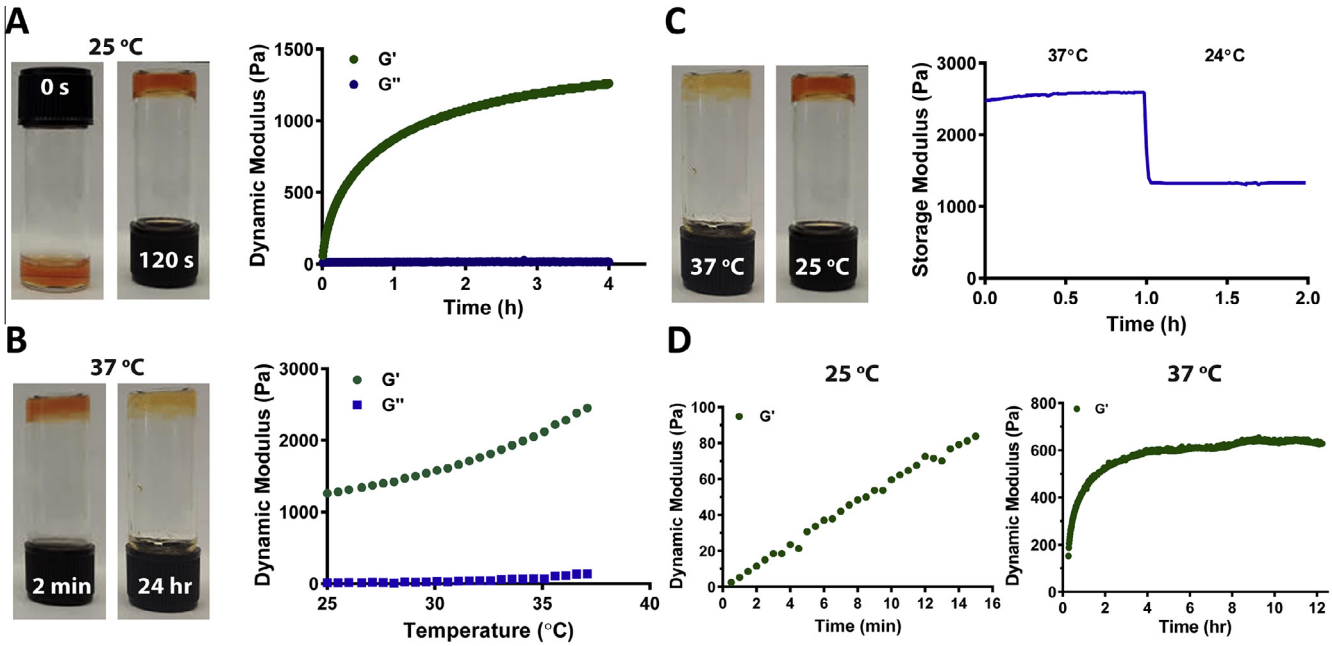

Fig. 2. The viscoelastic behavior of PNJ-Gelatin hydrogel solutions at (A) room temperature (25 °C for 4 h), followed by measuring during controlled (0.5 °C/min) and (B) sustained heating (37 °C for 1 h), and finally during (C) rapid cooling back to room temperature (25 °C for 1 h). (D) Changes in storage modulus of the PNJ-Gelatin hybrid hydrogel according to the temperature increase from 25 °C (preparation temperature) to 37 °C (incubation temperature). G′: storage modulus, G″: loss modulus.

assess alignment of F-actin fibers (Fig. 5A, FFT insets). There were no overall tissue-level alignment, however, numerous local alignment were detected across both culture conditions. FFT images (dashed rectangles, subsets of 40× images in Fig. 5A) of small cell clusters illustrated the local cellular alignment. Additionally, the actin area coverage was analyzed within both culture conditions. As can be seen in Fig. 5B, a significant difference ($p < 0.05$) in terms of actin coverage was observed between the culture groups pointing to the contributions of CFs in assembling a dense cell organization in co-culture condition [50].

3.4. Analyses of cardiac-specific markers

Sarcomeric α-actinin, troponin I, and connexin 43 (cardiac-specific markers) were stained to assess cardiac cells phenotype within the PNJ-Gelatin biohybrid hydrogel. Fig. 6A represents the immunostained images of both mono- and co-culture groups at day 7. As can be seen in the co-culture images, the sarcomeric structures demonstrated defined, uniaxial, and extended arrangements. Moreover, a homogenous distribution pattern of connexin 43 was observed for co-culture in comparison to the disarrayed expression of these gap junctions in mono-culture condition. In addition, the fluorescence coverage area (Fig. 6B), correlating to the architecture and distribution of expressed cardiac proteins, was quantified based on 20× immunostained images. Sarcomeric α-actinin and connexin 43 displayed statistically (t-test (two tailed); $p < 0.05$) higher coverage area in co-culture condition. The cells exhibited a well distribution of troponin I in both culture conditions. Overall, the presence of CFs assisted CMs to connect and form cell–cell junctions (as indicated by connexin 43), producing well-distributed and connected clusters of cells.

To demonstrate that encapsulation and subsequent culture of cardiac cells within the PNJ-Gelatin hydrogel did not alter their gene expression profile, we performed QPCR analysis on day 1 and 7. This analysis revealed that there were no statistically significant (t-test (two tailed); $p > 0.05$) changes in expression of CMs specific genes including cTNT, MLC2v, ACTN1, and CX43 in both the mono- and co-culture condition over the course of 7 days of culture (Fig. 7).

3.5. Beating behavior of the encapsulated cardiac cells

Beating behavior of cardiac cells was examined by analyzing the number of tissue-level (2.5×2.5 mm^2 field of view) synchronous contraction in a daily manner. The results in Fig. 8A and B show the average number of beats per minute (BPM) within both mono- and co-culture groups. In mono-culture, the encapsulated cardiac cells started beating individually on day 3 (supplementary Movie MS1). As the cells came into contact with each other, they demonstrated a synchronized beating behavior starting at day 6 of culture (57 ± 19 BPM) (Fig. 8A; supplementary Movie MS2). These observations were consistent with network formation of the cells based on the phase contrast and fluorescence images (Fig. 4B). The BPM reached the highest value (92 ± 42 BPM, $p < 0.05$) on day 7 followed by a significant decline to 36 ± 28 BPM by day 9. Additionally, the beating behavior was not maintained uniformly over the culture period (unstable trend represented by the blue line). On the other hand, the co-culture group (Fig. 8B) exhibited synchronous beating as early as day 3 of culture (39 ± 20 BPM) (supplementary Movie MS3 and MS4) and maintained a stable trend (represented by the blue line) in terms of BPM up to day 9 (30 ± 8 BPM) (supplementary Movie MS5).

To further investigate contraction signal synchrony in terms of amplitude and frequency, the tissue-level field of view (2.5×2.5 mm^2) was subdivided in to 0.5×0.5 mm^2 subsets. Fig. 8C and D show beating signals of subsets within a single representative field of view. As can be seen, the mono-culture signals displayed high fluctuations in peak to peak amplitude and period whereas co-culture condition exhibited uniform signals. Furthermore, similar frequencies between subset signals were observed for co-culture, whereas such behavior was not seen in mono-culture of the CMs. These findings indicated that the different subset areas within one field of view for the co-culture group were in synchrony compared to the mono-culture condition.

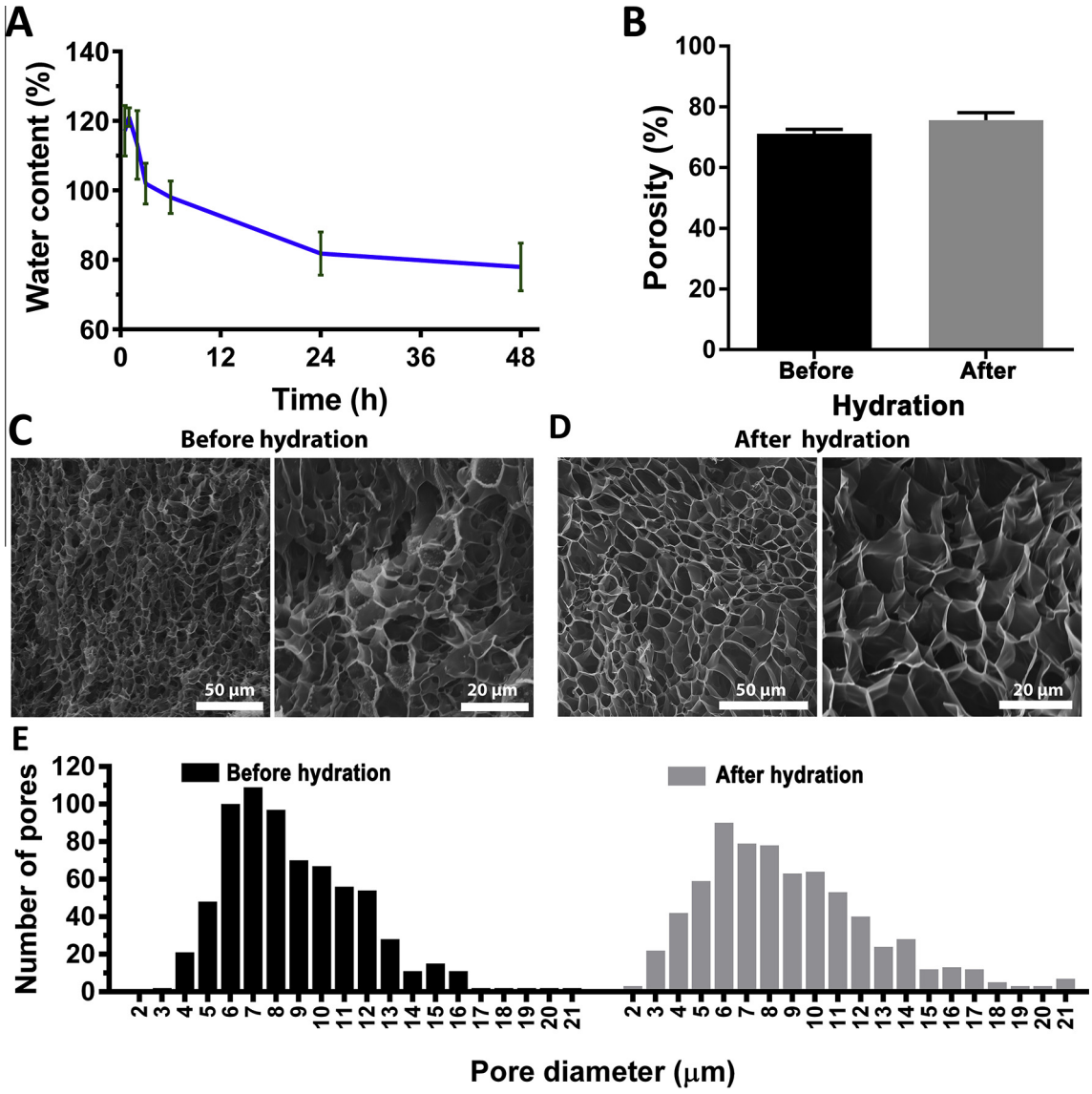

Fig. 3. The physical characteristics of PNJ-Gelatin hydrogel. (A) The change in the water content level (%) of the hydrogel during 48 h of hydration. (B) The percent of void structure (porosity) (%), (C) and (D) Low and high magnification SEM micrographs showing macroporous architecture, and (E) pore size distribution of lyophilized hydrogel before and after hydration (24 h).

Moreover, amplitude and frequency variation indexes were developed to further quantitatively analyze the tissue-level synchrony. Amplitude and frequency variations were found to be significantly lower in co-culture compared to mono-culture, indicating higher tissue-level synchrony in the co-culture condition (Fig. 8E and F).

3.6. External electrical stimulation

To investigate the response of encapsulated CMs and CFs within the PNJ-Gelatin hydrogel to external electrical stimulation, samples were treated by pulsatile electrical signals at day 7. Supplementary Fig. S3 shows the assembled chamber and the excitation threshold for both mono- and co-culture groups. Despite lower excitation threshold for the co-culture of the cells, no significant differences were detected between the two culture groups for the applied frequencies (1, 2, and 3 Hz). In addition, only individual areas within the hydrogel samples responded to the external electrical field, and started to contract.

4. Discussion

Although current hydrogels provide a desirable matrix for the delivery of exogenous cells to the infarct region, the majority of developed biomaterials suffer from well-tuned properties such as lack of cell-adhesion motifs [39,56,57] or robust mechanical properties [30,31]. Particularly, a large body of the previous work on injectable hydrogels has been concentrated on animal studies without extensive *in vitro* analyses on functionalities of cardiac cells to define an optimal culture condition [36,58–60]. Moreover, most of the earlier studies focused on the use of only CMs rather than co-culture conditions with CFs, being the most abundant cell within the myocardium after CMs [45]. For instance, Li et al. [36] utilized carbon nanotube (CNT) modified PNIPAAm for cardiac regeneration applications. They performed minimal *in vitro* studies prior to *in vivo* work, demonstrating that the presence of CNTs significantly promoted cellular adhesion and spreading. In another study by Wall et al. [58], semi-interpenetrating hydrogels of p(NIPAAm)-co-Polyacrylic acid (pAAc) hydrogels with matrix metalloproteinase (MMP) labile crosslinkers were developed for

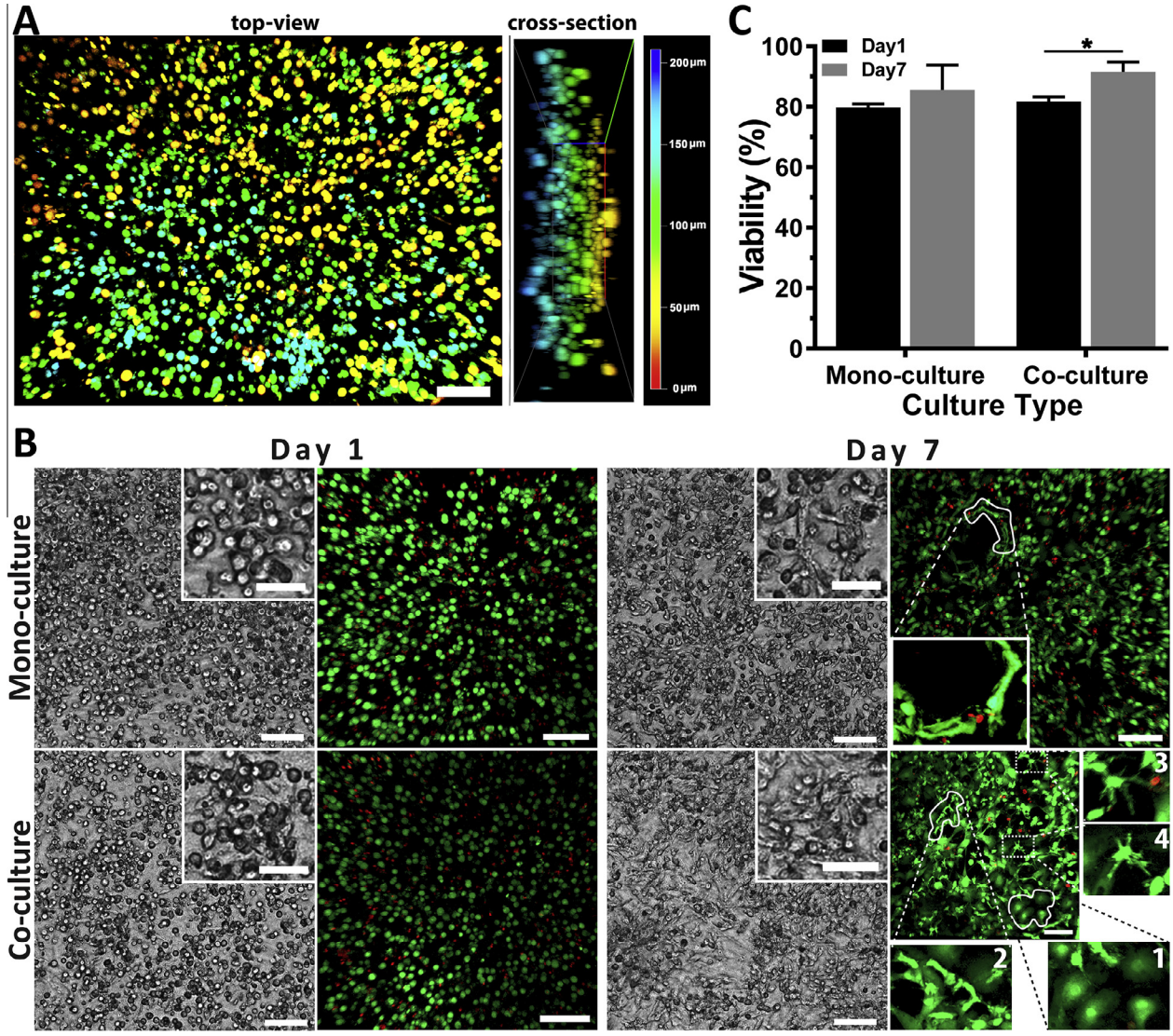

Fig. 4. The 3D tissue construct and subsequent cytotoxicity assessment of the hydrogel. (A) The depth coding image (scale bar represents 100 µm) of encapsulated cardiac cells within PNJ-Gelatin hydrogel (top-view & cross-section) confirming the formation of a 3D tissue construct (day 1). (B) The phase-contrast (scale bars represent 100 µm) and fluorescent images (green {live} and red {dead}) of mono- and co-culture groups illustrating cell morphology at days 1 and 7 of culture. Insets on phase-contrast (scale bars represent 50 µm) and stained images show the magnified images (inset #1 and 2 show CFs and CMs respectively; inset #3 and 4 display small protrusions in CMs). (C) Quantified viability (%) of both mono- and co-cultured groups at days 1 and 7. ($n = 3$; $^{*}p < 0.05$). (For interpretation of the references to color in this figure legend, the reader is referred to the web version of this article.)

transplantation of bone marrow-derived mesenchymal stem cells (BMSCs) and treatment of cardiac injuries. Cellular proliferation was investigated within the proposed matrices, as a function of mechanical stiffness and RGD concentration, to select a suitable matrix prior to *in vivo* work. Cui et al. [59] presented an injectable matrix using PolyNIPAM-based copolymers and electroactive tetraaniline (TA) for transplantation of rat cardiac myoblast within the infarct region. They performed material characterization and viability testing before animal studies. Wagner's group [60] also developed a copolymer made of N-isopropylacrylamide (NIPAAm), acrylic acid (AAc) and hydroxyethyl methacrylate-poly (trimethylene carbonate) (HEMAPTMC) (poly(NIPAAm-co-AAc-co-HEMAPTMC)) for cardiac regeneration upon myocardial infarction. They performed extensive characterizations to define the optimal monomer ratios with respect to gelation, solubility and degradation of the material. *In vitro* viability studies (rat vascular smooth muscle cells) was performed prior to *in vivo* testing. Therefore, it is crucial to perform extensive *in vitro* analyses on cardiac function before continuing to *in vivo* experimentation. Likewise, there is a critical need to discover whether the synthesized injectable hydrogel will accommodate the resident CFs within the infarct region as well as determining the subsequent influences of CFs on tissue-level functionalities.

In this work, a biohybrid injectable hydrogel was developed from gelatin and PNIPAAm-based copolymers to address these limitations. Gelatin, a naturally-derived biomaterial, was chosen to provide a suitable microenvironment with high bioactivity for cell growth and spreading [13–15,24], while PNIPAAm was selected to induce physical crosslinking and obtain sufficient mechanical robustness for the accommodation of dynamic tissue-level beating [34–36]. The synthesized hydrogel provided a dual-crosslinkable matrix, where the thiols and acrylates initiated a chemical gelation along with a secondary physical crosslinking to induce mechanical enhancement. The rheology results (Fig. 2) supported the chemical and physical crosslinking nature of the PNJ-Gelatin injectable hydrogel. Because the standard rheology approach may not

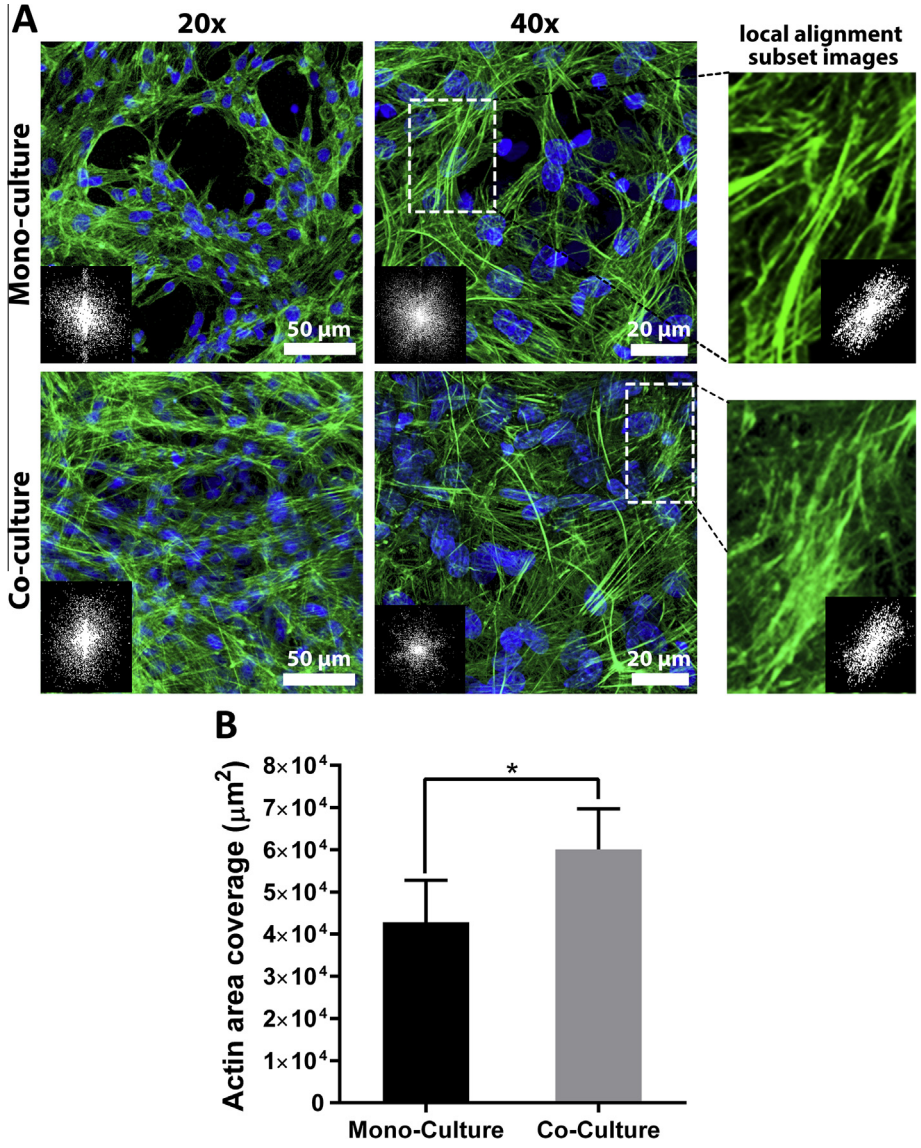

Fig. 5. The cytoskeleton organization and analysis of F-actin fiber alignment within PNJ-Gelatin hydrogel. (A) F-actin fibers (green) stained images in both culture groups representing the cytoskeleton organization at 20× and 40× magnifications; FFT images (inset) indicate fiber alignment within the formed 3D cardiac tissue. The magnified spots and related inset FFT images illustrate the local alignment of F-actin fibers. (B) The average coverage area (μm^2) of the F-actin fibers at day 7 of culture ($n > 10$; $^{*}p < 0.05$). (For interpretation of the references to color in this figure legend, the reader is referred to the web version of this article.)

represent the exact biophysical cues that the cells feel during the sample preparation, we devised a simple test to simulate the viscoelastic behavior of the biohybrid hydrogel with cells during the initial 12 h of culture. As seen in Fig. 2D, the cells experienced the chemical crosslinking first, followed by the hydrogel physical crosslinking once the samples were placed inside the incubator. However, these results still may not fully represent the actual biophysical cues, due to many other factors that influence the final modulus, such as hydrogel swelling, degradation, and ECM deposition [61].

The ECM-like macroporous structures, provided by PNJ-Gelatin hydrogels, make these types of biomaterials a desirable candidate for cell growth. Typically, PNIPAAm-based hydrogels exhibit low water content equilibrium, which can limit nutrient and gas exchange within the hydrogel structure [39]. To that regard, gelatin and JAAm were included as the key components within the PNJ-Gelatin hydrogel, which consequently resulted in enhanced water retention [41]. After hydration, the porous structures of the hydrogel increased slightly, indicating the retention of water (Fig. 3B). The difference in the water content can be equated to the hydrogel porous structures becoming more uniform and open (Fig. 3D) along with the increase in the range of pore diameters (Fig. 3E). Therefore, the material characterizations ensured suitable and tunable properties for cellular delivery based on the natural/synthetic nature of the proposed hydrogel matrix.

An ideal cell delivery hydrogel needs to provide a suitable microenvironment to enhance cardiac cell biological functions and promote cell survival, spreading, cytoskeletal organization, and specific markers expression [11,62]. The PNJ-Gelatin was used to encapsulate two different cell culture systems (CMs and 2:1 CMs–CFs) to assess the performance of the synthesized hydrogel for cardiac tissue engineering. We used 2:1 culture ratio based on our earlier optimization studies [50]. In this work, both culture groups demonstrated high cell viability and spreading within the 3D PNJ-Gelatin hydrogel (Fig. 4). These findings can be attributed to the high bioactivity of gelatin [24,38], adequate pore size distribution, and water content [43], which are required for sufficient cell infiltration and nutrition, waste, and gas exchange within the

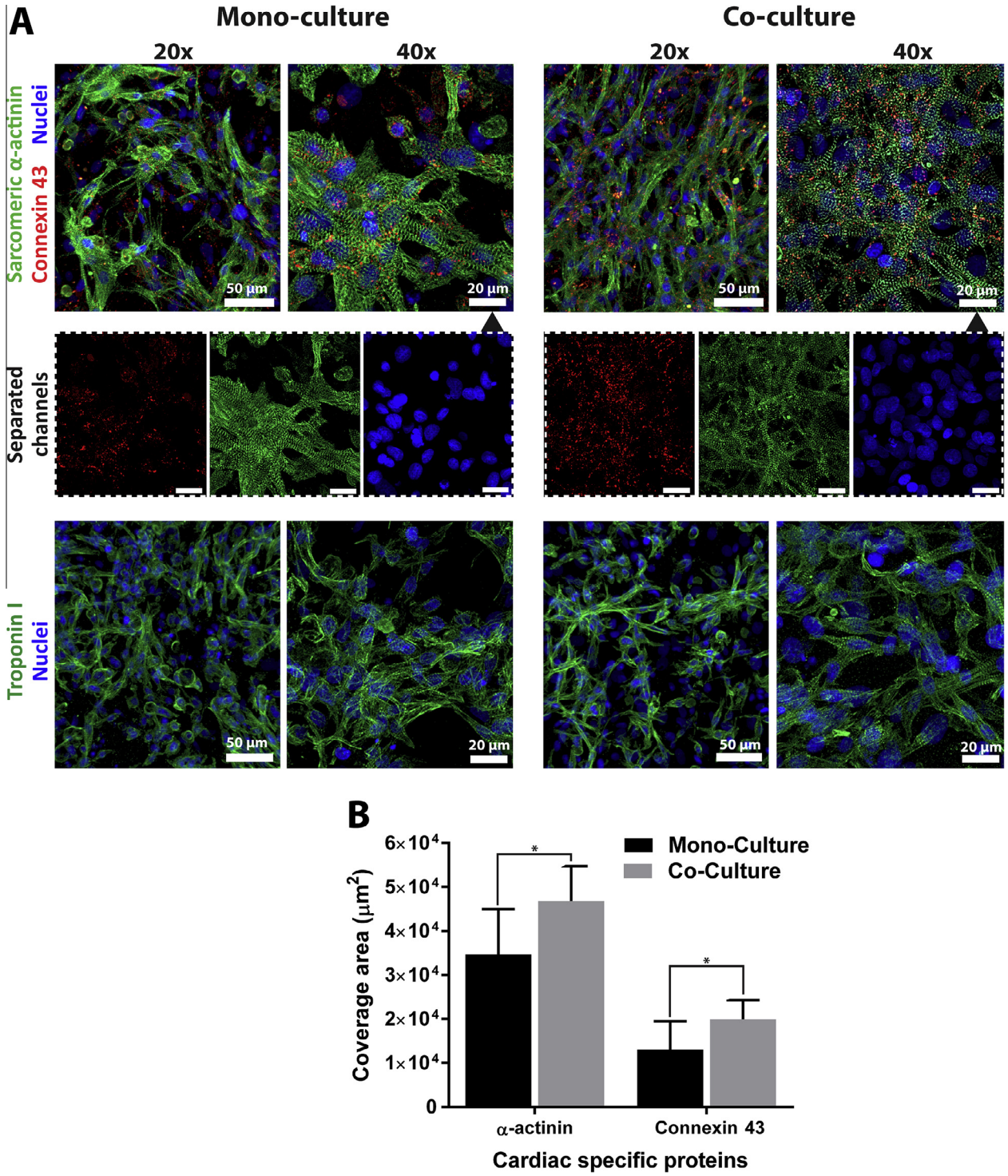

Fig. 6. Immunostaining and structural distribution of cardiac specific markers in both culture groups within PNJ-Gelatin hydrogel. (A) The immunostained images (day 7) of mono- and co-culture groups illustrating the structure and distribution of sarcomeric α-actinin, troponin I, and connexin 43 at two different magnifications (20×, 40×). (B) The average coverage area (μm^2) of sarcomeric α-actinin and connexin 43 proteins at day 7 ($n > 12$; $^*p < 0.05$).

3D ($10 \times 10 \times 0.2\ mm^3$) matrix. The co-culture group exhibited a significant increase in viability by day 7 which can be associated to the highly proliferative nature of CFs [45]. This is also reflected in the day 7 images (Fig. 4B) of co-culture, where there appeared to be a network of elongated cells located between the round cells. The findings from the viability and cell spreading analyses could be attributed to the incorporation of a highly bioactive component (gelatin) within the otherwise synthetic, PNIPAAm-based hydrogel. Gelatin not only provided sufficient cell adhesion motifs, but it also offered a high level of bioactivity as well as inducing high water retention that was overall missing in PNIPAAm. In addition, we performed hydrolytic degradation of the hydrogel. Our data indicated a sharp decrease in the molecular mass after 1 day, but the trend stabilized for the next few weeks (supplementary Fig. S4). We concluded that this decrease was not degradation, but uncrosslinked products being released from the material. Nonetheless,

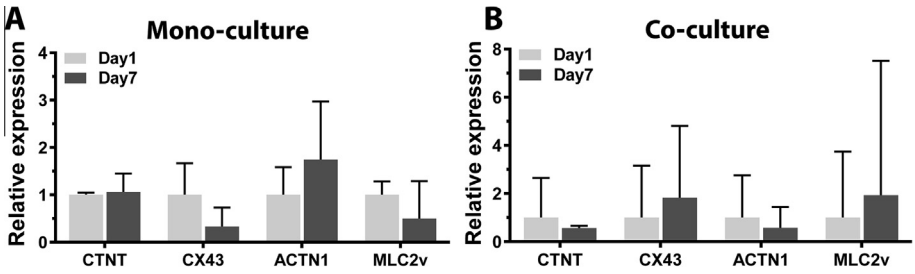

Fig. 7. Evaluation of the cardiac specific gene expression within PNJ-Gelatin hydrogel. The expression level of CTNT, CX43, ACTN1, and MLC2v genes at two different time points (day 1 and 7) for (A) mono-culture and (B) co-culture.

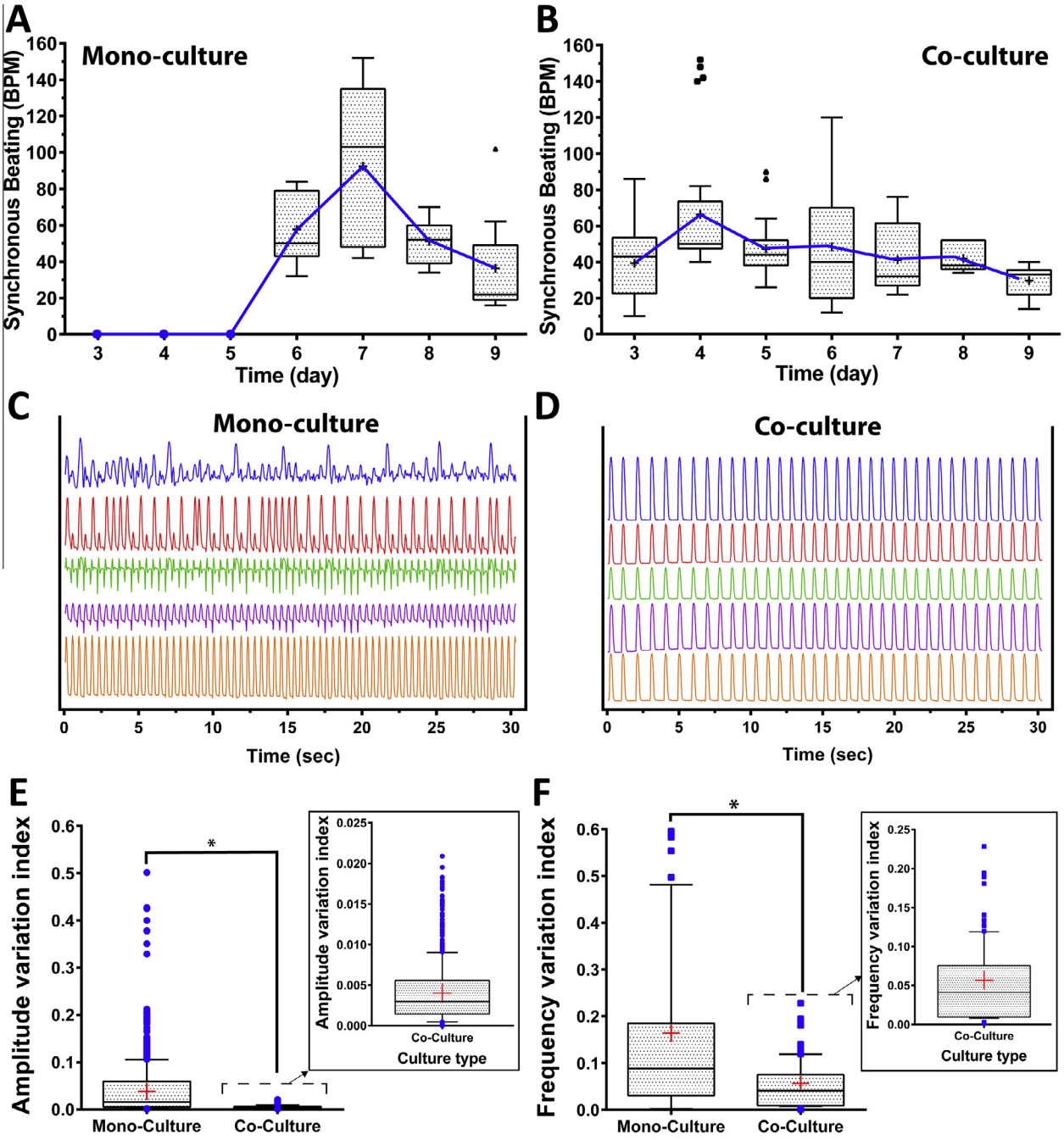

Fig. 8. Tissue-level beating and synchrony assessment of cultured cardiac cells within the PNJ-Gelatin hydrogel. The average number of beats per minute (BPM) for (A) mono- and (B) co-culture groups from day 3 to 9 of culture. (C) and (D) represent beating signals of five different subsets (0.5×0.5 mm^2) within hydrogel sample (2.5×2.5 mm^2) at day 7. The quantified (E) amplitude and (F) frequency variations represented as indexes comparing the synchrony of beating for mono- and co-culture groups.

gelatin was able to be degraded enzymatically [24], but the PNIPAAm-based components did not contain any degradable monomers. After enzymatic degradation, it was expected that LCST would have increased due to gelatin chains breaking down and separating the NIPAAm components resulting in NIPAAm units with short hydrophilic gelatin tails. In addition, the increase in LCST beyond physiological temperatures means that the polymer may become soluble within the body and cleared. However, the molecular weight of the byproducts was not investigated and may result in toxicity if too high. For future work, our group has a plan to improve the degradability of the PNJ-Gelatin hydrogel by incorporation of biodegradable components from our previous studies [41].

The resulting cell specific characteristics (Figs. 5–7) and functionalities (Fig. 8) within the PNJ-Gelatin highlighted the potential of the proposed hydrogel as an efficient and bioactive cardiac cell delivery system and further revealed the dissimilarities between the two investigated cell culture conditions (CM and 2:1 CM–CF). First of all, phenotypic differences in the distribution and structures of cytoskeleton and cardiac specific proteins were observed across both cultured cell systems (Figs. 5 and 6). The presence of CFs can be accredited to these differences by providing structural support as well as mechanical, electrical, and biochemical cues [45,61]. Primarily, distribution of F-actin, sarcomeric α-actinin, and connexin 43 proteins in co-culture were more uniformly organized contrary to the discrete arrangement in mono-culture. In this regard, CFs may have enhanced cell–cell and cell-ECM mechanical interactions by amplifying the availability of cadherin- and integrin-based anchoring points as demonstrated in our and other previous works [50,61,63,64]. This resulted in enhanced spreading of cardiac cells, which increased the coverage area of F-actin (Fig. 5B) and sarcomeric α-actinin (Fig. 6B). Furthermore, CFs facilitate cell–cell electrical coupling by contributing connexin 43 gap junctions [65–67], which is reflected by the homogenous distribution (Fig. 6A, 40×) and higher coverage area in co-culture condition (Fig. 6B). Secondly, qPCR analysis revealed that encapsulation and subsequent culture of CMs, either alone or with CFs, in the PNJ-Gelatin hydrogel had no effect on their gene expression profile. Third, incorporation of CFs with CMs gave rise to a dramatic difference in beating behavior, which correlates to cardiac cell and tissue functions [45,68]. We have observed that as CMs reached to each other and formed clusters of cells as they began to contract. However, such behavior was more pronounced in the presence of CFs, as helper cells. To that regard, the mechanical and electrical signaling provided by the CFs was speculated to induce higher cell–cell coupling [61,63,65,67], which resulted in earlier tissue-level contractions, as well as relatively stable average BPM in co-culture condition (Fig. 8A and B). In addition, the CFs engaged in signal propagation within the formed cardiac tissue, as demonstrated by the synchronous contraction signals (Fig. 8C and D) taken from the different areas ($0.5 \times 0.5\ mm^2$) of a single hydrogel sample ($2.5 \times 2.5\ mm^2$). Such behavior was also quantitatively represented as amplitude and frequency variation indexes, which determined tissue-level ($2.5 \times 2.5\ mm^2$) synchrony (Fig. 8E and F). The mono-culture group mostly demonstrated asynchronous beating fashion, which can cause low action potential signal propagation upon injection within the host myocardium. These observations are indeed consistent with our previous work on the development of micro-tissues embedded with the co-cultures of the CMs and CFs (with optimized ratio of 2:1) within a gelatin methacrylate (GelMA) hydrogel [50]. However, CMs in mono-culture did not spread or exhibit any spontaneous contraction in GelMA hydrogel. Such differences further indicated that the proposed hydrogel exhibits superior properties and can be used as a suitable matrix to supports cardiac cells functionalities in both mono-culture and co-culture conditions. The influence of paracrine signaling between CMs and CFs is subject of our future studies. Furthermore, we intend to test the *in vivo* functionalities of the cell-embedded hydrogel matrix in our future work.

External electrical stimulation setup (supplementary Fig. S3) was employed to assess the response of cardiac cells to the electrical stimulation. Both mono- and co-culture groups reacted to the applied stimulation similarly and no significant differences were observed. Furthermore, the inclusion of CFs in co-culture, which resulted to a significant synchronous contraction compared to the mono-culture condition, did not facilitate the propagation of external electrical pulses throughout the hydrogel constructs.

5. Conclusions

In this study, we synthesized PNJ-Gelatin hydrogel as an injectable matrix for cardiac cells delivery and tissue engineering applications. The proposed material featured chemical crosslinking to combine gelatin to the thermo-responsive PNIPAAm in a time dependent manner to induce a mechanically robust injectable hydrogel. Furthermore, incorporation of gelatin and JAAm into the hydrogel offered bioactivity and higher water content leading to excellent cell survival, adhesion, spreading, cytoskeletal and cardiac specific markers organization. The two cultured groups within the PNJ-Gelatin hydrogel demonstrated desirable phenotypic and functional outcomes, which illustrated the potential of the injectable matrix for cardiac tissue engineering and cell delivery applications. In addition, the synthesized matrix was able to home CFs (often found within the infarct region) to enhance the overall functionalities of the cell-embedded hydrogel. Particularly, the co-culture group exhibited higher synchronous tissue-level contractions, which could be attributed to the structural and distribution differences of cardiac specific markers (sarcomeric α-actinin and connexin 43) as well as cytoskeleton organization (F-actin fibers).

Acknowledgments

The monoclonal antibody, TI-4, developed by Stefano Schiaffino was purchased from the Developmental studies Hybridoma Bank, created by NICHD of the NIH and maintained at The University of Iowa, Department of Biology, Iowa City, IA 52242. We gratefully acknowledge the use of facilities with the LeRoy Eyring Center for Solid State Science at Arizona State University. Also, we acknowledge Harpinder Saini for helping for cell isolation, and Ryan. T. Sullivan and Nathan Moore for the analyses of beating data.

Appendix A. Supplementary data

Supplementary data associated with this article can be found, in the online version, at http://dx.doi.org/10.1016/j.actbio.2015.12.019.

References

[1] H.B. Wang, J. Zhou, Z.Q. Liu, C.Y. Wang, Injectable cardiac tissue engineering for the treatment of myocardial infarction, J. Cell. Mol. Med. 14 (2010) 1044–1055.
[2] J. Leor, S. Aboulafia-Etzion, A. Dar, L. Shapiro, I.M. Barbash, A. Battler, Y. Granot, S. Cohen, Bioengineered cardiac grafts – a new approach to repair the infarcted myocardium?, Circulation 102 (2000) 56–61
[3] H. Reinecke, C.E. Murry, Taking the death toll after cardiomyocyte grafting: a reminder of the importance of quantitative biology, J. Mol. Cell. Cardiol. 34 (2002) 251–253.
[4] J. Muller-Ehmsen, P. Whittaker, R.A. Kloner, J.S. Dow, T. Sakoda, T.I. Long, P.W. Laird, L. Kedes, Survival and development of neonatal rat cardiomyocytes transplanted into adult myocardium, J. Mol. Cell. Cardiol. 34 (2002) 107–116.
[5] W.H. Zimmermann, R. Cesnjevar, Cardiac tissue engineering: implications for pediatric heart surgery, Pediatr. Cardiol. 30 (2009) 716–723.
[6] K.L. Christman, R.J. Lee, Biomaterials for the treatment of myocardial infarction, J. Am. Coll. Cardiol. 48 (2006) 907–913.

[7] W.N. Lu, S.H. Lu, H.B. Wang, D.X. Li, C.M. Duan, Z.Q. Liu, T. Hao, W.J. He, B. Xu, Q. Fu, Y.C. Song, X.H. Xie, C.Y. Wang, Functional improvement of infarcted heart by co-injection of embryonic stem cells with temperature-responsive chitosan hydrogel, Tissue Eng. Part A 15 (2009) 1437–1447.
[8] J.L. Ifkovits, E. Tous, M. Minakawa, M. Morita, J.D. Robb, K.J. Koomalsingh, J.H. Gorman, R.C. Gorman, J.A. Burdick, Injectable hydrogel properties influence infarct expansion and extent of postinfarction left ventricular remodeling in an ovine model, Proc. Natl. Acad. Sci. U.S.A. 107 (2010) 11507–11512.
[9] M.-N. Giraud, A.G. Guex, H.T. Tevaearai, Cell therapies for heart function recovery: focus on myocardial tissue engineering and nanotechnologies, Cardiol. Res. Pract. 2012 (2012). Article ID 971614, 10 pages.
[10] S. Fernandes, S. Kuklok, J. McGonigle, H. Reinecke, C.E. Murry, Synthetic matrices to serve as niches for muscle cell transplantation, Cells Tissues Organs 195 (2012) 48–59.
[11] A. Hasan, A. Khattab, M.A. Islam, K.A. Hweij, J. Zeitouny, R. Waters, M. Sayegh, M.M. Hossain, A. Paul, Injectable hydrogels for cardiac tissue repair after myocardial infarction, Adv. Sci. 2 (2015) 2198–3844.
[12] J. Cutts, M. Nikkhah, D.A. Brafman, Biomaterial approaches for stem cell-based myocardial tissue engineering, Biomark. Insight (2015) 77–90.
[13] J.M. Singelyn, K.L. Christman, Modulation of material properties of a decellularized myocardial matrix scaffold, Macromol. Biosci. 11 (2011) 731–738.
[14] H.P. Tan, K.G. Marra, Injectable, biodegradable hydrogels for tissue engineering applications, Materials 3 (2010) 1746–1767.
[15] G.D. Nicodemus, S.J. Bryant, Cell encapsulation in biodegradable hydrogels for tissue engineering applications, Tissue Eng. Part B-Rev. 14 (2008) 149–165.
[16] K.L. Christman, A.J. Vardanian, Q.Z. Fang, R.E. Sievers, H.H. Fok, R.J. Lee, Injectable fibrin scaffold improves cell transplant survival, reduces infarct expansion, and induces neovasculature formation in ischemic myocardium, J. Am. Coll. Cardiol. 44 (2004) 654–660.
[17] J.H. Ryu, I.K. Kim, S.W. Cho, M.C. Cho, K.K. Hwang, H. Piao, S. Piao, S.H. Lim, Y.S. Hong, C.Y. Choi, K.J. Yoo, B.S. Kim, Implantation of bone marrow mononuclear cells using injectable fibrin matrix enhances neovascularization in infarcted myocardium, Biomaterials 26 (2005) 319–326.
[18] K.L. Christman, H.H. Fok, R.E. Sievers, Q.H. Fang, R.J. Lee, Fibrin glue alone and skeletal myoblasts in a fibrin scaffold preserve cardiac function after myocardial infarction, Tissue Eng. 10 (2004) 403–409.
[19] E.J. Suuronen, J.P. Veinot, S. Wong, V. Kapila, J. Price, M. Griffith, T.G. Mesana, M. Ruel, Tissue-engineered injectable collagen-based matrices for improved cell delivery and vascularization of ischemic tissue using $CD133^{+}$ progenitors expanded from the peripheral blood, Circulation 114 (2006) I138–I144.
[20] I. Kutschka, I.Y. Chen, T. Kofidis, T. Arai, G. von Degenfeld, A.Y. Sheikh, S.L. Hendry, J. Pearl, G. Hoyt, R. Sista, P.C. Yang, H.M. Blau, S.S. Gambhir, R.C. Robbins, Collagen matrices enhance survival of transplanted cardiomyoblasts and contribute to functional improvement of ischemic rat hearts, Circulation 114 (2006) I167–I173.
[21] W.D. Dai, S.L. Hale, G.L. Kay, A.J. Jyrala, R.A. Kloner, Delivering stem cells to the heart in a collagen matrix reduces relocation of cells to other organs as assessed by nanoparticle technology, Regen. Med. 4 (2009) 387–395.
[22] T. Kofidis, J.L. de Bruin, G. Hoyt, D.R. Lebl, M. Tanaka, T. Yamane, C.P. Chang, R. C. Robbins, Injectable bioartificial myocardial tissue for large-scale intramural cell transfer and functional recovery of injured heart muscle, J. Thoracic Cardiovasc. Surg. 128 (2004) 571–578.
[23] S.H. Lu, H.B. Wang, W.N. Lu, S. Liu, Q.X. Lin, D.X. Li, C. Duan, T. Hao, J. Zhou, Y.M. Wang, S.R. Gao, C.Y. Wang, Both the transplantation of somatic cell nuclear transfer- and fertilization-derived mouse embryonic stem cells with temperature-responsive chitosan hydrogel improve myocardial performance in infarcted rat hearts, Tissue Eng. Part A 16 (2010) 1303–1315.
[24] K. Nakajima, J. Fujita, M. Matsui, S. Tohyama, N. Tamura, H. Kanazawa, T. Seki, Y. Kishino, A. Hirano, M. Okada, R. Tabei, M. Sano, S. Goto, Y. Tabata, K. Fukuda, Gelatin hydrogel enhances the engraftment of transplanted cardiomyocytes and angiogenesis to ameliorate cardiac function after myocardial infarction, PLoS ONE 10 (2015).
[25] N. Annabi, K. Tsang, S.M. Mithieux, M. Nikkhah, A. Ameri, A. Khademhosseini, A.S. Weiss, Highly elastic micropatterned hydrogel for engineering functional cardiac tissue, Adv. Funct. Mater. 23 (2013) 4950–4959.
[26] M. Kharaziha, M. Nikkhah, S.R. Shin, N. Annabi, N. Masoumi, A.K. Gaharwar, G. Camci-Unal, A. Khademhosseini, PGS: gelatin nanofibrous scaffolds with tunable mechanical and structural properties for engineering cardiac tissues, Biomaterials 34 (2013) 6355–6366.
[27] C. Ceccaldi, S.G. Fullana, C. Alfarano, O. Lairez, D. Calise, D. Cussac, A. Parini, B. Sallerin, Alginate scaffolds for mesenchymal stem cell cardiac therapy: influence of alginate composition, Cell Transplantation 21 (2012) 1969–1984.
[28] M. Shevach, R. Zax, A. Abrahamov, S. Fleischer, A. Shapira, T. Dvir, Omentum ECM-based hydrogel as a platform for cardiac cell delivery, Biomed. Mater. 10 (2015).
[29] S.B. Seif-Naraghi, J.M. Singelyn, M.A. Salvatore, K.G. Osborn, J.J. Wang, U. Sampat, O.L. Kwan, G.M. Strachan, J. Wong, P.J. Schup-Magoffin, R.L. Braden, K. Bartels, J.A. DeQuach, M. Preul, A.M. Kinsey, A.N. DeMaria, N. Dib, K.L. Christman, Safety and efficacy of an injectable extracellular matrix hydrogel for treating myocardial infarction, Sci. Transl. Med. 5 (2013) 173ra25.
[30] N.H. Romano, D. Sengupta, C. Chung, S.C. Heilshorn, Protein-engineered biomaterials: nanoscale mimics of the extracellular matrix, BBA-Gen. Subj. 1810 (2011) 339–349.
[31] L. Little, K.E. Healy, D. Schaffer, Engineering biomaterials for synthetic neural stem cell microenvironments, Chem. Rev. 108 (2008) 1787–1796.
[32] M.E. Davis, J.P.M. Motion, D.A. Narmoneva, T. Takahashi, D. Hakuno, R.D. Kamm, S.G. Zhang, R.T. Lee, Injectable self-assembling peptide nanofibers create intramyocardial microenvironments for endothelial cells, Circulation 111 (2005) 442–450.
[33] C.C. Huang, H.J. Wei, Y.C. Yeh, J.J. Wang, W.W. Lin, T.Y. Lee, S.M. Hwang, S.W. Choi, Y.N. Xia, Y. Chang, H.W. Sung, Injectable PLGA porous beads cellularized by hAFSCs for cellular cardiomyoplasty, Biomaterials 33 (2012) 4069–4077.
[34] T. Wang, D.Q. Wu, X.J. Jiang, X.Z. Zhang, X.Y. Li, J.F. Zhang, Z.B. Zheng, R.X. Zhuo, H. Jiang, C.X. Huang, Novel thermosensitive hydrogel injection inhibits post-infarct ventricle remodelling, Eur. J. Heart Fail. 11 (2009) 14–19.
[35] L. Cai, R.E. Dewi, S.C. Heilshorn, Injectable hydrogels with in situ double network formation enhance retention of transplanted stem cells, Adv. Funct. Mater. 25 (2015) 1344–1351.
[36] X. Li, J. Zhou, Z.Q. Liu, J. Chen, S.H. Lu, H.Y. Sun, J.J. Li, Q.X. Lin, B.G. Yang, C.M. Duan, M. Xing, C.Y. Wang, A PNIPAAm-based thermosensitive hydrogel containing SWCNTs for stem cell transplantation in myocardial repair, Biomaterials 35 (2014) 5679–5688.
[37] X.J. Jiang, T. Wang, X.Y. Li, D.Q. Wu, Z.B. Zheng, J.F. Zhang, J.L. Chen, B. Peng, H. Jiang, C.X. Huang, X.Z. Zhang, Injection of a novel synthetic hydrogel preserves left ventricle function after myocardial infarction, J. Biomed. Mater. Res. A 90a (2009) 472–477.
[38] J.M. Heffernan, D.J. Overstreet, L.D. Le, B.L. Vernon, R.W. Sirianni, Bioengineered scaffolds for 3D analysis of glioblastoma proliferation and invasion, Ann. Biomed. Eng. 43 (2015) 1965–1977.
[39] J.M. Heffernan, D.J. Overstreet, S. Srinivasan, L.D. Le, B.L. Vernon, R.W. Sirianni, Temperature responsive hydrogels enable transient three-dimensional tumor cultures via rapid cell recovery, J. Biomed. Mater. Res. A 104 (2015) 17–25.
[40] H.G. Schild, Poly(N-isopropylacrylamide) – experiment, theory and application, Prog. Polym. Sci. 17 (1992) 163–249.
[41] D.J. Overstreet, R. Huynh, K. Jarbo, R.Y. McLemore, B.L. Vernon, In situ forming, resorbable graft copolymer hydrogels providing controlled drug release, J. Biomed. Mater. Res. A 101 (2013) 1437–1446.
[42] D.J. Overstreet, R.Y. McLemore, B.D. Doan, A. Farag, B.L. Vernon, Temperature-responsive graft copolymer hydrogels for controlled swelling and drug delivery, Soft Mater. 11 (2013) 294–304.
[43] N. Annabi, J.W. Nichol, X. Zhong, C.D. Ji, S. Koshy, A. Khademhosseini, F. Dehghani, Controlling the porosity and microarchitecture of hydrogels for tissue engineering, Tissue Eng. Part B-Rev. 16 (2010) 371–383.
[44] D.L. Elbert, J.A. Hubbell, Conjugate addition reactions combined with free-radical cross-linking for the design of materials for tissue engineering, Biomacromolecules 2 (2001) 430–441.
[45] C.A. Souders, S.L.K. Bowers, T.A. Baudino, Cardiac fibroblast the renaissance cell, Circ. Res. 105 (2009) 1164–1176.
[46] B.H. Lee, B. West, R. McLemore, C. Pauken, B.L. Vernon, In-situ injectable physically and chemically gelling NIPAAm-based copolymer system for embolization, Biomacromolecules 7 (2006) 2059–2064.
[47] K.P. Vercruysse, D.M. Marecak, J.F. Marecek, G.D. Prestwich, Synthesis and in vitro degradation of new polyvalent hydrazide cross-linked hydrogels of hyaluronic acid, Bioconjugate Chem. 8 (1997) 686–694.
[48] X.Z. Shu, Y.C. Liu, F. Palumbo, G.D. Prestwich, Disulfide-crosslinked hyaluronan-gelatin hydrogel films: a covalent mimic of the extracellular matrix for in vitro cell growth, Biomaterials 24 (2003) 3825–3834.
[49] G.L. Ellman, Tissue sulfhydryl groups, Arch. Biochem. Biophys. 82 (1959) 70–77.
[50] H. Saini, A. Navaei, A. Van Putten, M. Nikkhah, 3D cardiac microtissues encapsulated with the co-culture of cardiomyocytes and cardiac fibroblasts, Adv. Healthc. Mater. 4 (2015) 1961–1971.
[51] S.R. Shin, S.M. Jung, M. Zalabany, K. Kim, P. Zorlutuna, S.B. Kim, M. Nikkhah, M. Khabiry, M. Azize, J. Kong, K.T. Wan, T. Palacios, M.R. Dokmeci, H. Bae, X.W. Tang, A. Khademhosseini, Carbon-nanotube-embedded hydrogel sheets for engineering cardiac constructs and bioactuators, ACS Nano 7 (2013) 2369–2380.
[52] H.D. VanGuilder, K.E. Vrana, W.M. Freeman, Twenty-five years of quantitative PCR for gene expression analysis, Biotechniques 44 (2008) 619–626.
[53] N. Tandon, C. Cannizzaro, P.H.G. Chao, R. Maidhof, A. Marsano, H.T.H. Au, M. Radisic, G. Vunjak-Novakovic, Electrical stimulation systems for cardiac tissue engineering, Nat. Protoc. 4 (2009) 155–173.
[54] Z. Cui, B. Lee, B.L. Vernon, A new hydrolysis-dependent thermosensitive polymer for an injectable degradable drug delivery system, Biomacromolecules 8 (2007) 1280–1286.
[55] A.V. Sigel, M. Centrella, M. EghbaliWebb, Regulation of proliferative response of cardiac fibroblasts by transforming growth factor-beta(1), J. Mol. Cell. Cardiol. 28 (1996) 1921–1929.
[56] L. Jongpaiboonkit, W.J. King, G.E. Lyons, A.L. Paguirigan, J.W. Warrick, D.J. Beebe, W.L. Murphy, An adaptable hydrogel array format for 3-dimensional cell culture and analysis, Biomaterials 29 (2008) 3346–3356.
[57] J.A. Hunt, R. Chen, T. van Veen, N. Bryan, Hydrogels for tissue engineering and regenerative medicine, J. Mater. Chem. B 2 (2014) 5319–5338.
[58] S.T. Wall, C.C. Yeh, R.Y.K. Tu, M.J. Mann, K.E. Healy, Biomimetic matrices for myocardial stabilization and stem cell transplantation, J. Biomed. Mater. Res. A 95a (2010) 1055–1066.
[59] H.T. Cui, Y.D. Liu, Y.L. Cheng, Z. Zhang, P.B. Zhang, X.S. Chen, Y. Wei, In vitro study of electroactive tetraaniline-containing thermosensitive hydrogels for cardiac tissue engineering, Biomacromolecules 15 (2014) 1115–1123.
[60] K.L. Fujimoto, Z.W. Ma, D.M. Nelson, R. Hashizume, J.J. Guan, K. Tobita, W.R. Wagner, Synthesis, characterization and therapeutic efficacy of a

biodegradable, thermoresponsive hydrogel designed for application in chronic infarcted myocardium, Biomaterials 30 (2009) 4357–4368.
[61] I. Banerjee, K. Yekkala, T.K. Borg, T.A. Baudino, Dynamic interactions between myocytes, fibroblasts, and extracellular matrix, Ann. N.Y. Acad. Sci. 1080 (2006) 76–84.
[62] A. Paul, A. Hasan, H. Al Kindi, A.K. Gaharwar, V.T.S. Rao, M. Nikkhah, S.R. Shin, D. Krafft, M.R. Dokmeci, D. Shum-Tim, A. Khademhosseini, Injectable graphene oxide/hydrogel-based angiogenic gene delivery system for vasculogenesis and cardiac repair, ACS Nano 8 (2014) 8050–8062.
[63] P. Kohl, Heterogeneous cell coupling in the heart – an electrophysiological role for fibroblasts, Circ. Res. 93 (2003) 381–383.
[64] S.C. Baxter, M.O. Morales, E.C. Goldsmith, Adaptive changes in cardiac fibroblast morphology and collagen organization as a result of mechanical environment, Cell Biochem. Biophys. 51 (2008) 33–44.
[65] P. Camelliti, G.P. Devlin, K.G. Matthews, P. Kohl, C.R. Green, Spatially and temporally distinct expression of fibroblast connexins after sheep ventricular infarction, Cardiovasc. Res. 62 (2004) 415–425.
[66] P. Camelliti, T.K. Borg, P. Kohl, Structural and functional characterisation of cardiac fibroblasts, Cardiovasc. Res. 65 (2005) 40–51.
[67] L. Chilton, W.R. Giles, G.L. Smith, Evidence of intercellular coupling between co-cultured adult rabbit ventricular myocytes and myofibroblasts, J. Physiol.-Lond. 583 (2007) 225–236.
[68] T. Kaneko, F. Nomura, K. Yasuda, On-chip constructive cell-network study (I): contribution of cardiac fibroblasts to cardiomyocyte beating synchronization and community effect, J. Nanobiotechnol. 9 (2011).